Theory of band-population effects in electroreflectance

N. Bottka and David Linton Johnson*
Michelson Laboratory, Naval Weapons Center, China Lake, California 93555
(Received 1 October 1974)

A theory of band-population effects in electroreflectance is presented without invoking the usual Franz-Keldysh mechanism. The theory is based on the relative shift between the bands and the Fermi level when an external field is applied. Spatially varying relative Fermi level near the semiconductor surface and the effective-mass approximation to the bands are assumed when calculating the change in the dielectric function $\langle \Delta\epsilon \rangle$. Results are compared with experimentally observed structures in InSb and PbSe.

I. INTRODUCTION

Band population in semiconductor materials occurs when, under steady-state condition, the Fermi level E_F lies within the conduction- or valence-band states. This condition can occur either in the bulk of the material under heavy extrinsic doping or near its surface under heavy accumulation or inversion biasings. In either case, the band-population phenomenon manifests itself in optical measurements either as a shift in the fundamental absorption edge of the material as a function of doping (the Burstein-Moss shift[1,2]) or as a shift in electroreflectance (ER) structure of near-degenerate materials when the surface of the sample is biased into accumulation.[3]

We focus our attention on the latter phenomenon where band-population effects can be observed in ER not only at the fundamental edge of the material, but at all allowed interband transitions involving the unoccupied electronic states near the Fermi level. Figure 1 shows this schematically where, at equilibrium, for a given applied bias the Fermi level is constant throughout the crystal, but at each point near the surface the band population varies as one goes from the surface into the bulk. In the ER experiments light probes these differently populated levels, and the mechanism giving rise to ER structure is no longer a simple critical-point-associated phenomena. Indeed, for accumulation conditions at the surface (assuming completely degenerate conditions throughout the sample) the predominant mechanism of ER will be band-population modulation. It is this aspect of the problem we wish to address in this paper, namely, the calculation of the changes in the dielectric function of a material under band-population conditions and its relation to changes observed in electroreflectance.

In Sec. II we calculate the imaginary part of the dielectric function ϵ_2 under the constraint of the exclusion principle (Fermi-Dirac statistics) assuming a single-particle picture and quadratic surfaces in the energy bands, $E(\vec{k})$. For completeness, we treat both valence- to conduction-band and intervalence- and conduction-band transitions for both parabolic and hyperbolic band surfaces. (For convenience we consider heavily doped n-type materials). We follow by calculating the screening depth and the spatially varying potential near the surface of a nearly degenerate to degenerate semiconductor. Utilizing this spatial variation in band population within the space-charge region we calculate the averaged $\langle \Delta\epsilon \rangle$ over this region and finally obtain the normalized change in reflectance $\Delta R/R$.

In Sec. III we compare these theoretical results with experimentally obtained line shapes in InSb and PbSe and discuss the validity of the assumptions made. In Sec. IV we consider a specific case where both critical-point (Franz-Keldysh mechanism[4]) and band-population mechanisms contribute to the ER signal. We conclude in Sec. V by discussing the effect of space-charge-induced localized states on electroreflectance in near-degenerate materials. Section VI is a summary.

II. BAND-POPULATION MODULATION IN DEGENERATE SEMICONDUCTORS

A. Dielectric-function relation

The contribution to the imaginary part of the dielectric function $\epsilon_2(\hbar\omega)$ for photon-induced direct transitions between a valence and a conduction band takes the form[4] (nondegenerate bands)

$$\epsilon_2(\hbar\omega, E_F(z)) = [4\pi^2 e^2\hbar^2/m^2(\hbar\omega)^2][2/(2\pi)^3]\,|\hat{\epsilon}\cdot\vec{P}_{vc}|^2 \times \int d^3k\,\delta(E_{vc}(\vec{k})-\hbar\omega)\,f_v[1-f_c(E_F(z))], \quad (1)$$

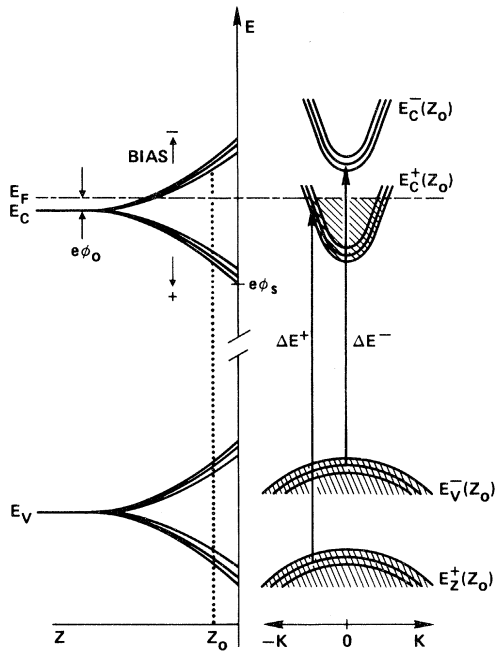

FIG. 1. Schematic showing the shift of the threshold energy ΔE at absolute zero for an optical transition as the bands of degenerate n-type InSb are shifted with respect to the Fermi level E_F by an applied bias. A valence band E_v and a conduction band E_c are shown as a function of depth z from the surface (left) and as a function of momentum K for an arbitrary depth z_0 about the Γ point (right). Modulation around a given bias is represented by the band-edge wobble. The symbols − and + represent the bias direction for a p- and n-type surface, respectively.

where the matrix element $\vec{P}_{vc}$ is assumed $\vec{k}$ independent. $E_F(z)$ is the Fermi energy with respect to the conduction band at any point z in the crystal and, in the space-charge region of a semiconductor, is given by (see Fig. 1)

$$E_F(z) = E_F + e\phi(z), \tag{2}$$

where $e\phi(z)$ is the potential energy of an electron in that region. $E_F(z)$ incorporates the shift of the bands relative to the constant Fermi level, E_F, under the action of an externally applied bias. f_v is the occupation probability of the initial state (assumed to be unity for valence--to--conduction-band transition in n-type materials) and $f_c(E_F)$ the final state, respectively. f_c is the Fermi-Dirac factor given by

$$f_c = (1 + e^{[E_c(\vec{k}) - E_F(z)]/kT})^{-1}. \tag{3}$$

We intend to apply Eq. (1) to highly doped n-type[5] narrow-gap semiconductors such that the dielectric screening length is much smaller than the effective Bohr radius of the impurity level. We may then assume that (i) there is no impurity level or band (this implies a temperature-independent Hall coefficient), and (ii) the electronic band structure is the same as for the intrinsic material but with the Fermi level raised considerably into the conduction band, reflecting the increased number of electrons. Note that we have so far neglected the Franz-Keldysh mechanism and have assumed that the dominant effect of the applied field is to shift the bands relative to the Fermi level as described by Eq. (2). See Sec. III for a discussion of this point.

Equation (1) can readily be solved in spherical coordinates for an isotropic M_0, M_3-type[4] of isoenergetic quadratic surfaces:

$$\epsilon_2(M_i) = C(|\mu|/m)^{3/2}(|\hat{\epsilon}\cdot\vec{P}_{vc}|^2/m) \times[(\pm\chi)^{1/2}/(\hbar\omega)^2]\, G_i(E_F)u(\pm\chi), \tag{4}$$

where

$$G_i(E_F) = (e^{D_i(E_F)} + 1)^{-1}, \tag{5}$$

$$D_i(E_F) = [E_F(z) \mp (|\mu|/m_c^*)\chi]/kT, \tag{6}$$

and

$$\chi = \hbar\omega - E_g. \tag{7}$$

m, μ, m_c^*, $u(\chi)$, and E_g are the electron mass, reduced mass, the conduction-band effective mass, the unit step function, and the critical-point gap energy, respectively. C is a numerical constant equal to $8\sqrt{(13.6)}$ if $\hbar\omega$ is in eV. The upper sign holds for M_i, $i=0$ ($\mu>0$), the lower sign for M_i, $i=3$ ($\mu<0$). Expression (4) describes the shift of the (threshold) edge with increasing conduction-band population (the Burstein-Moss shift[1,2]).

Since in many materials band population can occur at points in the Brillouin zone not at $\vec{k}=0$ we consider, for completeness, the anisotropic M_i, $i=0$, and M_i, $i=1$, type[4] of surfaces. Using cylindrical coordinates in (1) we obtain

$$\epsilon_2(M_i) = \pm C(\mu_T\mu_L^2/m^3)^{1/2}(|\hat{\epsilon}\cdot\vec{P}_{vc}|^2/m) \times[1/(\hbar\omega)^2]\int_0^{(\pm\chi)^{\frac{1}{2}}} dy\, N_i(y), \tag{8}$$

$$N_i(y) = (e^{Ay^2 + D_i} + 1)^{-1}, \tag{9}$$

$$A = (\mu_T/m_{cT}^* \mp |\mu_L|/m_{cL}^*)/kT, \tag{10}$$

$$D_0 = [E_F(z) - (\mu_T/m_{cT}^*)\chi]/kT, \tag{11}$$

$$D_i = [E_F(z) + (|\mu_L|/m_{cT}^*)\chi]/kT, \tag{12}$$

where the upper sign holds for $i=0$ (μ_T, $\mu_L>0$) and the lower sign for $i=1$ ($\mu_T>0$, $\mu_L<0$). μ_T (μ_L), m_{cT}^* (m_{cL}^*) are the transverse (longitudinal) reduced and conduction-band effective masses, respectively. Note that Eq. (8) reduces to the form of Eq. (4) for $\mu_L/m_{cL}^* = \mu_T/m_{cT}^*$ for a M_0 type of surface. In general Eq. (8) has no analytical form

and must be solved numerically.

We will consider specific examples of transitions from a lower-lying valence band to the lowest conduction band, in narrow-gap semiconductors. In those cases, by $\vec{k}\cdot\vec{p}$ perturbation theory,[6] the valence effective masses are each much larger in absolute value than the lowest conduction masses (where the lowest conduction to highest valence band gap is quite small) and so $\mu_L/m^*_{cL} = \mu_T/m^*_{cT} = 1$ and $A = 0$, and the integral of Eq. (8) reduces to the form of Eq. (4). This is true, for example, for the $L^+_{45} \rightarrow L^-_6$ transition in PbSe which we have checked numerically.

Since, for degenerate conditions, interconduction-band transitions are also possible,[7] we can write an expression similar to Eq. (4) for transitions from the lower conduction band to the next higher conduction band:

$$\epsilon_2(M_i) = C(|\mu|/m)^{3/2}(|\hat{\epsilon}\cdot\vec{P}_{cc'}|^2/m) \times[(\pm\chi)^{1/2}/(\hbar\omega)^2]\, H_i(E_F)u(\pm\chi), \quad (13)$$

where now the matrix element $\vec{P}_{cc'}$ involves the initial partially filled band c and the final state c'. Since $f_c \neq 1$ and $f_{c'} = 0$ we obtain

$$H_i(E_F) = (e^{J_i(E_F)} + 1)^{-1}, \quad (14)$$

$$J_i(E_F) = [\pm(|\mu|/m^*_c)\chi - E_F(z)]/kT, \quad (15)$$

where again the upper sign holds for $i = 0$ and the lower one for $i = 3$.

B. $\Delta\epsilon$ for a uniform band population

We can differentiate expression (4) with respect to the potential ϕ (see Fig. 1) and obtain, in effect, band-population modulation:

$$\Delta\epsilon_2(z) = \frac{d\epsilon_2}{d(e\phi)}\Delta[e\phi(z)] = e\epsilon_2'\Delta\phi$$
$$= C(|\mu|/m)^{3/2}(|\hat{\epsilon}\cdot\vec{P}_{vc}|^2/m)[(\pm\chi)^{1/2}/(\hbar\omega)^2] \times G_i'[E_F(z)]\, u(\pm\chi)\Delta[e\phi(z)], \quad (16)$$

$$G_i'(E_F) = -(kT)^{-1} e^{D_i}/(e^{D_i}+1)^2. \quad (17)$$

D_i and its sign convention are the same as in Eq. (6). Similar expressions hold for interconduction-band transitions.

Figure 2 shows the line shapes of $\Delta\epsilon_2/e\Delta\phi$ for an $i = 0$ type of surface at 200°K for different values of $E_F + e\phi$. Also shown is $\Delta\epsilon_1/e\Delta\phi$ as obtained from Kramers-Kronig analysis.[4] Note the blue shift (Burstein-Moss shift) of the structure with increasing bias. This explains qualitatively the blue shift of the Γ_7-Γ_6 transitions in the ER structure in InSb observed by Glosser *et al.*[3]

Since the probing light penetrates the space-charge region it samples different levels of band

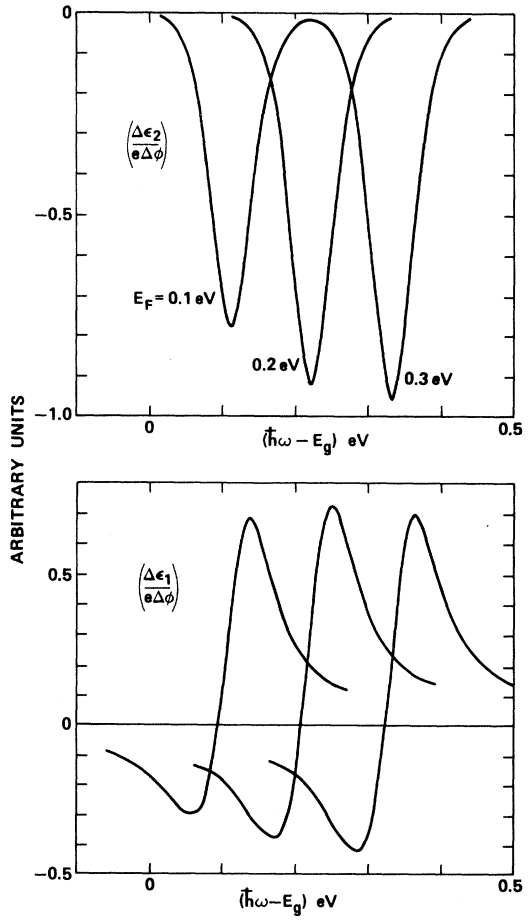

FIG. 2. Normalized change in the imaginary part $\Delta\epsilon_2/e\Delta\phi$ and the real part $\Delta\epsilon_1/e\Delta\phi$ of the dielectric function ϵ vs photon energy $\hbar\omega - E_g$ assuming uniform band population and isotropic quadratic isoenergetic surfaces. The calculation was done for InSb, at $T = 200$°K, $m^*_c = 0.012m$, $m^*_v = 0.11m$, and relative Fermi level $E_F(z) = E_F + e\phi(z)$ of 0.1, 0.2, and 0.3 eV, respectively. Equation (16) was used in calculating $\Delta\epsilon_2/e\Delta\phi$ and from it $\Delta\epsilon_1/e\Delta\phi$ was calculated by Kramers-Kronig analysis.

population. Consequently, for a quantitative comparison between theory and experiment we must know the screening depth and the distribution of the band population near the surface. We treat these subjects in Sec. II C and II D.

C. Screening length for degenerate semiconductors

At $T \neq 0$, for a parabolic conduction band, the bulk charge density n_0 is given by[8]

$$n_0 = (1/2\pi^2)(2m^*_c kT/\hbar^2)^{3/2}\int_0^\infty dy\,(y)^{1/2}/(e^{y-\gamma}+1)$$
$$= 2N_c F_{1/2}(\gamma)/(\pi)^{1/2}, \quad (18)$$

where $F_{1/2}(\gamma)$ is the Fermi-Dirac integral[8] and $\gamma = E_F/kT$. For a single parabolic band, n_0 is

identical to $1/R_H ec$, where R_H is the Hall coefficient assumed to be temperature independent.[9] R_H is therefore used to determine n_0 and thus E_F.

As regards screening, the Poisson relation takes the form

$$\nabla^2\phi(z) = 4\pi e[n(z) - n_0]/\epsilon_s \sim [F_{1/2}(\zeta) - F_{1/2}(\gamma)], \tag{19}$$

where $\zeta = \gamma + e\phi(z)/kT$ and ϵ_s is the static dielectric constant of the intrinsic material. In contrast to the classical Boltzman-statistics treatment of the Poisson relation,[10] Eq. (19) cannot be solved analytically; one can expand it and keep the linear term

$$\nabla^2\phi(z) = e^2[(2m_c^*)^3 kT]^{1/2} F_{-1/2}(\gamma)\phi(z)/(\pi\epsilon_s\hbar^3) = \phi(z)/\lambda^2, \tag{20}$$

where we can define a screening length λ by

$$\lambda = \{\pi\epsilon_s\hbar^3/e^2[(2m_c^*)^3 kT]^{1/2} F_{-1/2}(\gamma)\}^{1/2}, \tag{21}$$

which is the Debye length at high temperature (or low doping) and is the Thomas-Fermi screening length for $E_F/kT \to +\infty$. We intend our formalism to apply to degenerate semiconductors in which E_F ($\lesssim$0.1 eV) may be comparable to kT at 300°K (0.025 eV). Since the surface-barrier-electroreflectance (SBER) experiments use the metal-oxide-semiconductor (MOS) configuration, the solution to Eq. (20) in the bulk of the semiconductor has the form

$$\phi(z) = \phi_s\, e^{-|z|/\lambda}, \tag{22}$$

where ϕ_s is the potential at the oxide-semiconductor interface referred to zero in the bulk (the semiconductor thickness is much larger than λ). Equation (22) is equivalent to linear dielectric screening with a dielectric constant $\epsilon(q) = \epsilon_s\,[1 + 1/(\lambda q)^2]$.[11] We can go one step further and calculate the relationship between the gate voltage V_G and the surface potential,[10] thus establishing the relationship needed in Eqs. (2) and (22) for calculating the contribution from each point z near the surface to the total ER signal $\Delta R/R$. This turns out to be a linear relation in our approximation:

$$V_G - V_{FB} = [1 + (\epsilon_s/\epsilon_{ox})(t_{ox}/\lambda)]\,\phi_s. \tag{23}$$

Here V_{FB} is the flat-band voltage (it is a function of surface-state charges, assumed unchanged by bias, plus the difference of the work functions[10]), ϵ_s the intrinsic semiconductor dielectric constant, and ϵ_{ox} and t_{ox} the dielectric constant and thickness of the oxide, respectively. Relations (22) and (23) are strictly valid near flat band ($\phi_s = 0$); they may be assumed to be approximately valid even for $|\phi_s| \gtrsim E_F$.

D. $\Delta\epsilon$ for nonuniform band population

In order to include the band-population variation within the space-charge region, we use the nonuniform-field relation derived by Aspnes and Frova[12]:

$$\langle\Delta\epsilon\rangle = -2iK \int_{z_d \to -\infty}^{0} dz'\, e^{-2iKz'}\,\Delta\epsilon(z'), \tag{24}$$

where

$$\Delta\epsilon = \Delta\epsilon_1 + i\Delta\epsilon_2, \tag{25}$$

$$\Delta\epsilon_i(z) = \frac{d\epsilon_i}{d\phi}\, e^{-|z|/\lambda}\Delta\phi_s, \quad i = 1, 2 \tag{26}$$

$$K = (n + i\kappa)\omega/c. \tag{27}$$

n, κ, and c are the refractive index, extinction coefficient, and the speed of light, respectively. The phase factor in $e^{-2iKz'}$ mixes the real and imaginary parts of $\Delta\epsilon(z')$ thus strongly modifying the line shapes of $\langle\Delta\epsilon_1\rangle$ and $\langle\Delta\epsilon_2\rangle$ relative to those of Fig. 2 and thus $\Delta R/R$ as obtained from the uniform-field relation, i.e.,

$$e^{-2iKz'} = e^{i|z'|/a}\, e^{-|z'|/b}, \tag{28}$$

where b now is the penetration length of light and has the value $\hbar c/2\kappa\hbar\omega = 986.4/(\hbar\omega)\kappa$ Å; a is a measure of the mixing in $\Delta\epsilon$ and has the value $986.4/(\hbar\omega)n$ Å. Note that if a, b, and λ (screening length) are of comparable magnitude then the integral in Eq. (23) must be solved in its entirety. Only if $b \gg \lambda$ and $a \gg \lambda$ will the exponential [Eq. (28)] be slowly varying over the range of integration and can it be assumed constant, in which case the real and imaginary parts of $\Delta\epsilon$ will interchange.[12]

Assuming the exponential decay in the potential derived in (20), we obtain

$$\langle\Delta\epsilon\rangle = -2i(\omega/c)(n + i\kappa)\Delta v_s\lambda \times \int_0^1 dx\,\{\cos[2\omega n\lambda(\ln x)/c] - i\sin[2\omega n\lambda(\ln x)/c]\} \times x^{2\kappa\lambda\omega/c}(\epsilon_1' + i\epsilon_2'), \tag{29}$$

where $\Delta v_s = e\Delta\phi_s$, $\epsilon_2'(\hbar\omega, v_s x) = d\epsilon_2/dv$, the integration variable is $x = e^{z/\lambda} = \phi(z)/\phi_s$, and

$$\epsilon_1'(\hbar\omega, v_s x) = (2/\pi)P \times \int_0^\infty \omega'\epsilon_2'(\hbar\omega', v_s x)/(\omega'^2 - \omega^2)\,d\omega'. \tag{30}$$

The normalized change in reflectance $\Delta R/R$ can now be calculated from[13]

$$\Delta R/R = \mathrm{Re}[-(2\,n_a\,n_s D)^{-1}\langle\Delta\epsilon\rangle], \quad (31)$$

where n_a and n_s are the reflective indices of the ambient and the substrate material, respectively. D completely describes the effect of surface layers on the substrate and it is related to the generalized Seraphin coefficients α and β by[13]

$$\alpha - i\beta = -(2\,n_a\,n_s D)^{-1}. \quad (32)$$

Relation (29) is general insofar as it applies to any mechanism giving rise to change in ϵ provided the potential distribution within the space-charge region decays exponentially. It turns out that the line shape of $\langle\Delta\epsilon\rangle$ does not depend strongly on the detail of this potential decay, but only on v_s and λ.[14] In calculating $\Delta R/R$ in Sec. III we will use the expressions from (16) for ϵ_2' in (29) and (30).

III. COMPARISON WITH EXPERIMENT

We have presented the simplest possible theory having a reasonable chance of interpreting the ER experimental data in narrow-gap semiconductors. We have done so in order to focus our attention on this particular mechanism of electroreflectance. Despite its simplicity, there is a total of 12 independent parameters whose values must be determined in order to calculate $\Delta R/R$ vs $\hbar\omega$. Moreover, we must do numerical integrations over two variables for each $\hbar\omega$. Before we refine the theory, it therefore behooves us to compare the predictions of this theory with some experimental results on degenerate semiconductors. Before doing so it is wise to explicitly, but briefly, state and attempt to justify the assumptions we have made.

(i) The validity of the one-electron theory of solids and of the random-phase-approximation (RPA)[11] dielectric function for the contribution of the transitions in question to $\epsilon(\omega)$.

(ii) The validity of linear dielectric screening within the RPA vis-à-vis Eqs. (19)–(23). The linear approximation is strictly valid only near flat-band ($\phi_s \approx 0.0$) and we will consider situations in which $|e\phi_s| > E_F$. One of us (N.B.) has previously verified through numerical integration of the equivalent exact expressions on nondegenerate (classical statistics) doped semiconductors that $\Delta R/R$ is most insensitive to the approximations in Eqs. (19)–(23) as long as ϕ_s and λ are correctly determined.[14] The RPA formalism is an asymptotically exact approximation to $\epsilon(q)$ whenever $r_s < 1$,[11] which can easily be seen to be the case in most situations of interest.

(iii) The electronic band structure for the doped material is the same as that for the intrinsic material but with the excess carriers residing solely in the conduction or valence band (as the case may be). In particular, we assume that we are on the metallic side of the Mott transition so that the impurity levels or bands are screened; this will occur when λ is less than the impurity Bohr radius. A necessary condition is that the Hall coefficient be temperature independent.

(iv) The critical-point structure is adequately described by simple $\vec{k}\cdot\vec{p}$ theory, i.e., parabolic bands with constant matrix elements.

(v) We have completely neglected the Franz-Keldysh mechanism of electroreflectance. This mechanism is appreciable only within ~0.1 eV of the critical point; we will consider doping levels such that $E_F \sim 0.1$ eV and biased into accumulation so that this approximation may be expected to be valid. Moreover, the sharpness of the critical point is washed out by the impurity scattering. Nonetheless, for low doping and/or depletion biasing the remnant of the Franz-Keldysh mechanism must be included. Note that band-population modulation depends locally on the potential and has structure near $\hbar\omega \sim E_g + E_F(z)$ whereas the Franz-Keldysh mechanism depends locally on the electric field and has structure near $\hbar\omega \sim E_g$.

Band-population effects in ER were first reported by Glosser and Seraphin[3] (GS). Their experiments were done on n-type InSb. Unfortunately, some of the parameters needed in the analysis were not determined by them at that time. GS interpret structure around 1.1 eV as due to the Γ_7-Γ_6 transition (the "spin-orbit-split" valence band to lowest conduction band). In order to satisfy assumptions (ii), (iii), and (v) we wish to consider a relatively highly doped sample, biased into accumulation. However, according to Kane,[15] if $n \gtrsim 10^{18}$ cm^{-3} the conduction band becomes appreciably nonparabolic near E_F. We were able to obtain a spectrum for an n-type sample of InSb with $n = 1.0\times10^{17}$ cm^{-3} (the Hall coefficient is independent of temperature from 77 to 300°K) and have listed the pertinent parameters of the experiment in the caption to Fig. 3 (along with certain derived parameters). We actually used the continuously changing values of n, κ, α, β[16] of a two-phase substrate-ambient system in the 1.0-eV region. The "oxide" layer was achieved by anodizing the InSb in KOH. GS estimated the thicknesses of all their films to be about 300 Å; according to Hung and Yon[17] the dielectric constant of the resultant oxide is about 16. The flat-band voltage was not determined; we have very arbitrarily used the value reported by GS for a different sample. In principle V_{FB} can be determined as that gate voltage where the electroreflectance signal from a transition

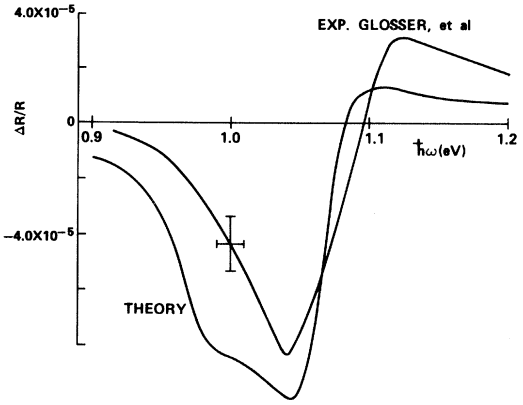

FIG. 3. Comparison between the experimentally observed $\Gamma_7-\Gamma_6$ structure in electroreflectance by Glosser *et al.* in InSb and the theoretically calculated line shape using Eqs. (29)–(31) and band-population modulation. The material parameters used in the calculation were as follows: $n_0=1.0\times10^{17}$ cm^{-3}, $T=77$°K, $m_c^*=0.012m$, $m_v^*=0.110m$, $E_F=0.055$ eV, matrix element $|\hat{e}\cdot\vec{P}_{vc}|^2/m=3.96$ eV, $E_g=0.90$ eV, refractive index $n=4.4$, extinction coefficient $\kappa=0.3$, penetration length of light $b=3000$ Å, screening length $\lambda=193$ Å, static dielectric constants of the oxide and InSb $\epsilon_{ox}=16$ and $\epsilon_s=17.8$, respectively, thickness of oxide $d=300$ Å, flat-band voltage of the MOS $V_{FB}=+0.25$ V, and gate and surface voltages $V_G=0.5$ V and $V_s=0.092$ V, respectively.

bridging the Fermi level inverts polarity.[3]

The resultant calculation is plotted in Fig. 3 with the experimental results supplied to us by Glosser. The value for E_g was chosen to be 0.9 eV.[18] As the experimental parameters were not well determined (the insulating layer may even be slightly conductive) we chose not to pursue this material further except to note the following: (i) The scale of the ordinate is as determined directly from our calculation; it is approximately of the right size for an electroreflectance signal, thus showing that, at the very least, this mechanism makes a non-negligible contribution to $\Delta R/R$. The experimental curve was then scaled so that the peak-to-peak heights agreed, as we did not know the scale of the experiment. (ii) The width of the spectrum agrees well with the experimental results. That the spectral shapes are in rough agreement is probably fortuitous as will be seen shortly.

We also calculated spectra corresponding to larger biases and found that our signal shifts to the blue with increasing gate voltage more readily than did the experimental signal, thus indicating that V_{FB} may well be large and negative (this would also tend to obviate the necessity for using a lower value of E_g) or that the position of the bands at the oxide-semiconductor interface is otherwise pinned. We suggest that further experimental and theoretical studies on InSb ($n\sim10^{17}-10^{18}$) in which V_{FB} has been experimentally determined and using a well-parametrized oxide layer (such as evaporated Al_2O_3), will be most fruitful.

Recently, Kinoshita and Glosser[19] (KG) performed the same experiment on n-type (1.0×10^{18} cm^{-3}) PbSe. In Fig. 4 we present their results for three different biases at 10°K, using an Al_2O_3 oxide layer. They identify this structure as arising from the $L_{45}^+(4)\rightarrow L_6^-(6)$ transition. The spin-orbit-split "twin" appears at ~2.1 eV. In the caption of Fig. 5 we have listed all the pertinent parameters. The effective masses quoted are $(m_{\parallel}m_{\perp}^2)^{1/3}$ as per Eq. (8). KG were unable, at low temperatures, to invert the 1.6-eV structure which is presumably a Franz-Keldysh effect between two levels bridging the Fermi level. Evidently, $V_{FB}<-3$ V owing to a large density of surface states at the oxide-semiconductor interface; consequently all three curves correspond to an accumulation condition. In Fig. 5 we have plotted the theoretical $\Delta R/R$ vs $\hbar\omega$ for different values of the gate bias (we have chosen not to specify V_{FB}). In this calculation we have used the generalized α, β coefficients[13] of a four-phase (ambient, Ni,[20] Al_2O_3,[21] and PbSe[22]) system. Several features are apparent.

(i) The sizes of the theoretical curves are much larger than in Fig. 3. This is due to a larger matrix element and to the fourfold star of the L point. Evidently, this mechanism is even more important in PbSe than in InSb.

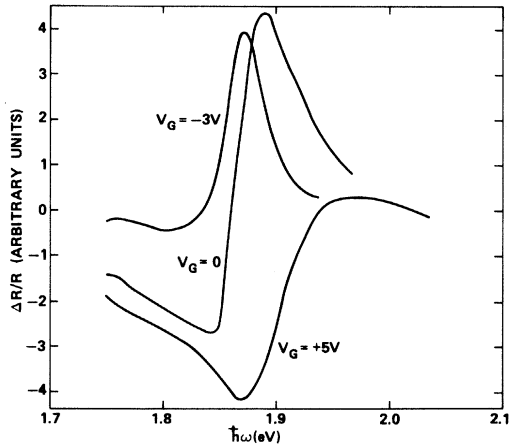

FIG. 4. Experimentally observed $L_{45}^+(4)-L_6^-(6)$ electroreflectance structures at 10°K in PbSe by Kinoshita and Glosser for an n-type, $n_0=1.0\times10^{18}$ cm^{-3} sample. The ER signal in the metal-insulator-semiconductor structure was measured as a function of dc bias $V_G=-3$, 0, 5 V, respectively.

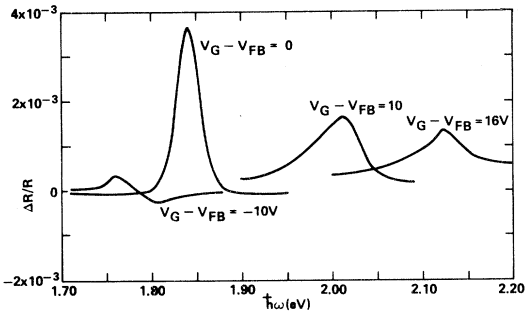

FIG. 5. Theoretically calculated line shapes of electroreflectance as a function of applied dc bias $V_G - V_{FB}$ for PbSe using Eqs. (29)–(31) and band-population modulation. The following material parameters were used in the calculation: $n_0 = 1.0 \times 10^{18}$ cm^{-3}, $T = 77$°K, $m_c^* = 0.040m$, $m_v^* = 0.218m$, $E_F = 0.076$ eV, matrix element $|\hat{\epsilon} \cdot \vec{P}_{vc}|^2/m = 50.3$ eV, $E_g = 1.75$ eV, refractive index $n = 4.4$, extinction coefficient $\kappa = 1.4$, penetration length of light $b = 361$ Å, screening length $\lambda = 280$ Å, thickness of the oxide $d = 200$ Å, static dielectric constants of the oxide and sample $\epsilon_{ox} = 3.12$ and $\epsilon_s = 280$, respectively.

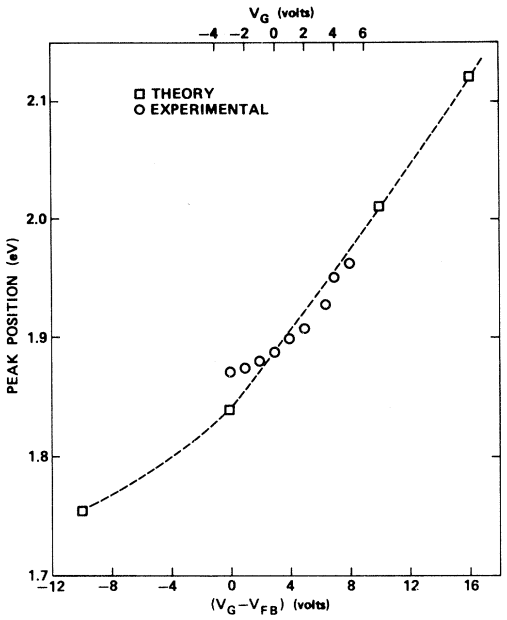

FIG. 6. Shift with gate bias voltage of the observed $L_{45}^{+}(4)$-$L_6^{-}(6)$ electroreflectance structure in PbSe from Fig. 4 and the theoretically calculated structure in Fig. 5. The abscissa was shifted in order to bring the two sets into line, corresponding to an arbitrary choice $V_{FB} = -3$ V in the theoretical curve.

(ii) Regardless of the choice of V_{FB}, the spectral shapes of the two sets will not agree. Tentatively, we attribute this drawback to imperfect knowledge of the required parameters, particularly of ϵ_s (PbSe). To the best of our knowledge this parameter, the truly static dielectric constant of intrinsic single-crystal PbSe at low temperatures, has not been measured directly and could conceivably be off by a factor of 5. Zemel[23] has used the Lyddane-Sachs-Teller relation to deduce ϵ_s, which therefore incorporates three different experimental errors. Error in ϵ_s is reflected in error in λ, which directly governs the mixing of the spectral shapes of Fig. 2 via the Aspnes-Frova relation (24). We notice that the band-population mechanism allows for a change of spectral shape with bias.

(iii) The spectral widths of the two sets are, as was the case for InSb, in more or less good agreement. The widths of each increase with bias and by roughly the same factor. This is to be expected from any mechanism from the Aspnes-Frova relationship. The theoretical width of $\Delta R/R$ vs $\hbar\omega$ is always larger than that at flat band, $V_G - V_{FB} = 0$, which is larger than kT because the modulating signal also decays into the bulk with decay length λ.

(iv) The band-population mechanism predicts a shift of structure to the blue with increased bias that is in quite excellent agreement with the experimental shift. In Fig. 6 we have plotted the position of the maximum in the theoretical curves as a function of $V_G - V_{FB}$, and likewise the positions of the experimental maxima vs V_G. We have shifted the abscissas in order to bring the two sets into line, corresponding to an arbitrary choice $V_{FB} = -3$ in the theoretical curves. The observed experimental shift ~0.1 eV over a range of 8 V in bias cannot, as previously noted, be explained by the Franz-Keldysh mechanism.

To conclude this section we emphasize the importance of accurate values for the required 12 parameters even for this, the simplest of all possible theories. In particular, one cannot theoretically interpret experimental results without a determination of V_{FB} which is sharply dependent on sample preparation, temperature, etc. Further experimental and theoretical investigations will be addressed to this problem.

IV. FRANZ-KELDYSH EFFECT IN DEGENERATE SEMICONDUCTORS

So far we have concentrated only on band-population mechanism giving rise to the observed structure in ER of heavily doped narrow-band semiconductors. We have assumed that E_F was far enough in the conduction band not to warrant the inclusion of critical-point effect, i.e., Franz-Keldysh effect. If E_F is near the bottom of the conduction band or if the effective electric field F involves an extended region in $\vec{k}$ space, then

we have to include the Fermi-Dirac factor in the general convolution relation of $\epsilon_2(\hbar\omega, F)$.[4] In general this relation is not readily solvable analytically. We can solve $\epsilon_2(\hbar\omega, F, E_F)$ for an M_0 critical point using the effective-mass approximation (EMA)[4] given by

$$\epsilon_2(\hbar\omega, F, E_F) = (4\pi^2 e^2 |\hat{\epsilon}\cdot\vec{P}_{cv}|^2/m^2\omega^2)(e^2|F_x F_y F_z|/\hbar^6\theta_x^2\theta_y^2\theta_z^2) \times \int_{-\infty}^{\infty} dE_x\, dE_y\, dE_z\, \mathrm{Ai}^2(-E_x/\hbar\theta_x)\,\mathrm{Ai}^2(-E_y/\hbar\theta_y)\,\mathrm{Ai}^2(-E_z/\hbar\theta_z) \times \delta(E_{vc}-\hbar\omega)(e^{[E_F-(\mu/m_c^*)(E_x+E_y+E_z)]/kT}+1)^{-1}, \quad (33)$$

where

$$E_{vc}(\vec{k}) = (\hbar^2/2\mu)\sum_i k_i^2 + E_g = E + E_g, \quad i = z, y, z \quad (34)$$

$$E_c(\vec{k}) = \mu E/m_c^*, \quad (35)$$

$$\theta_i^3 = e^2F_i^2/2\hbar\mu_i, \quad i = x, y, z \quad (36)$$

$$\theta^3 = e^2|F|^2/2\hbar\mu. \quad (37)$$

The first integration over the δ function brings the exponential term outside the integral. The other two integrals are readily solvable using integral relations for the Airy function.[4] Thus

$$\epsilon_2(\hbar\omega, F, E_F) = (B\theta^{1/2}/\omega^2)[|\mathrm{Ai}'(\eta)|^2 - \eta|\mathrm{Ai}(\eta)|^2] \times (e^{E_F-\mu/m_c^*\chi/kT}+1)^{-1} = \epsilon_2(\hbar\omega, F)G_0(E_F), \quad (38)$$

where

$$\eta = (\hbar\omega - E_g)/\hbar\theta = \chi/\hbar\theta. \quad (39)$$

B is a numerical constant,[4] and G_0 is given by (5).

The change in ϵ_2 is now

$$\Delta\epsilon_2(\hbar\omega, F, E_F) = [\epsilon_2'(\hbar\omega, F)G_0(E_F) + \epsilon_2(\hbar\omega, F)G_0'(E_F)]\Delta F, \quad (40)$$

where the prime indicates the derivative with respect to F. The physical meaning of (38) and (40) is apparent from Fig. 7, where the individual line shapes constituting $\epsilon_2(\hbar\omega, F, E_F)$ and $\Delta\epsilon_2(\hbar\omega, F, E_F)$ for a field-on/field-off case are shown. Note that for $E_F < 0$ (E_F in the gap), $G_0 = 1$ (constant), Eq. (40) reduces to the usual $\Delta\epsilon_2(\hbar\omega, F)$ line shape associated with the Franz-Keldysh mechanism.[4] For $E_F > 0$, the conduction band will populate and the G_0 term in (40) will tend to attenuate the pronounced structure in $\Delta\epsilon_2(\hbar\omega, F)$; i.e., there will be a suppression of the critical-point effect as E_F goes higher into the conduction band. In the limit that $E_F \gg \hbar\theta$ the critical-point effect will be completely suppressed and (40) reduces to $\epsilon_2(\hbar\omega, F)G_0'(E_F)\Delta F \approx \epsilon_2(\hbar\omega, 0)[dG_0/d(e\phi)] \times \Delta(e\phi)$, the band-population-modulation line shape derived in Sec. I.

Similar arguments hold for an M_3 critical point. Figure 7 shows this schematically for an interconduction-band transition where such an M_3 surface is most likely to occur because of $\vec{k}\cdot\vec{p}$ perturbation, i.e., $m_i^* < m_f^*$. In this case, when $E_F > 0$ critical-point transitions will be possible between the now populated initial state and the final state. $H_3 > 0$ for most of the significant structure in $\Delta\epsilon_2(\hbar\omega, F)$. As E_F moves higher up into the conduction band, band-population modulation will also become possible and, unlike the case of valence- to conduction-band transitions where

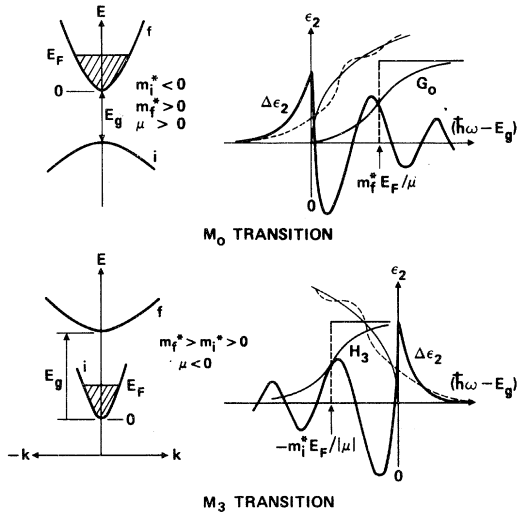

FIG. 7. Theoretical line shapes for $\epsilon_2(\hbar\omega, 0)$ (solid line), $\epsilon_2(\hbar\omega, F)$ (dashed line), and $\Delta\epsilon_2(\hbar\omega, F)$ for an M_0 and M_3 type of critical-point transition as obtained from Eqs. (38) and (40) when the Fermi level $E_F < 0$. The energy-band states $E(\vec{k})$ are shown on the left where E_g is the lowest (highest) energy difference between the initial (i) and final (f) state for an M_0 (M_3) transition. When $E_F > 0$, the above line shapes will be modified by the factors G_0 or H_3 (depending on the type of critical point) as given by Eqs. (14), (15), (38), and (40).

$E_F \gg \hbar\theta$ and only the second term in (40) dominated the line shape, now both the $\epsilon_2'(\hbar\omega, F)H_3(E_F)$ and $\epsilon_2(\hbar\omega, F)H_3'(E_F)$ terms in (40) will prevail. Note that the line shape of $\epsilon_2 H_3'$ will have a *red* shift as E_F increases (see Fig. 7). The chances of observing a M_3-critical-point transition as described above are good, provided we can swing the bands near the semiconductor surface from accumulation condition (thus band population) to depletion condition. The depletion-to-accumulation change in bias would allow the emergence of the M_3 structure in ER.

V. SPACE-CHARGE-INDUCED LOCALIZED STATES IN DEGENERATE SEMICONDUCTORS

The narrow, degenerate accumulation regions hereto considered will give rise to discrete energy levels within the potential well near the oxide-semiconductor interface[24, 25] (see Fig. 1) which we have ignored. These space-charge-induced localized states (for motion normal to the interface) in turn can give rise to structure in capacitance[26] or resonance absorption at far infrared.[27] We briefly discuss such effects in this section.

Our procedure has been to treat the wave functions in the space-charge region as if they were locally Bloch functions (this assumption violates the boundary conditions at the surface) and to use a potential derived from the linearized Thomas-Fermi theory. The inadequacies of this procedure can be seen most simply in the work of Baraff and Appelbaum[25] (BA) who also consider an accumulation region in a degenerate n-type semiconductor. In particular, we have ignored the likely existence of states whose motion normal to the surface is bound, and our potential is far from self-consistent. Our approximation to Figs. 9–11 of Ref. 25 consists of straight lines through the origin tangent to "Thomas-Fermi curve"; inasmuch as $r_s = 0.17$ for $n_0 = 10^{17}$ in InSb our treatment of the potential is seen to be in reasonable agreement with that of BA. Moreover, the transitions we have been considering involve states in the vicinity of E_F, which is to say, states in the continuum of the self-consistent potential, and our treatment of the wave functions can therefore also be expected to be approximately correct. It would be of interest to extend BA's work in the direction of our own.

We thought it informative to use the simple exponential potential given by Eq. (22) to calculate the eigenvalues associated with various bias voltages using Alferieff and Duke's relations.[28] For a typical Ni-Al_2O_3-InSb interface, $n_0 = 10^{17}$ cm^{-3}, for band bending of $e\phi_s = 0.175$ eV below the bulk conduction-band minimum the following eigenvalues emerge: $-E_i = 1.13$, 10.9, 34.7, 79.4 meV, respectively. In the above case the onset of a single quantized level occurs for $e\phi_s$ in the range 0–0.05 eV. Since we have assumed E_F to be above the bulk conduction-band minimum, all of these quantized states will be occupied and no photon-induced transitions to these states will be possible from the valence states. If the Fermi level is below the bulk conduction-band minimum (within the potential well), then transitions to the quantized states above the Fermi level can take place. It is unlikely that such transitions will be observed in electroreflectance (even at low temperatures) since the superposition of valence- to conduction-band transitions near the Fermi level will cover up their presence (it is to be noted that for points within the space-charge region where the Fermi level is within the conduction band, different regions of k space may be involved in the interband transition causing additional broadening in the ER structure). For degenerately doped semiconductors it may, however, be possible to observe these states vis-à-vis interconduction-band transitions in which the occupied bound levels are the initial states.

VI. SUMMARY AND CONCLUSIONS

We have presented the theoretical aspects of a new modulation mechanism which, we believe, gives rise to observed structure in surface-barrier electroreflectance in semiconductor materials. The theory is based on band-population effects within the space-charge region of a material, particularly in semiconductors having a narrow band gap. This mechanism differs considerably from the usual Franz-Keldysh critical-point-associated phenomenon, which is normally assumed to interpret electroreflectance structure. Theoretically calculated line shapes based on this mechanism explain reasonably well the salient features of electroreflectance structures observed in n-type InSb and PbSe (and which cannnot be explained by the usual Franz-Keldysh mechanism). Specifically, our calculation predicts (i) values for $\Delta R/R$ which are of the order of those generally observed experimentally, (ii) spectral linewidths in good agreement with those seen in InSb and PbSe and whose widths increase with bias in accordance with experimental observations, and, most importantly, (iii) a blue shift of structure (in PbSe) with increased bias in excellent agreement with experiment. Present lack of agreement of line shapes is traceable, in part, to imperfect knowledge of the required parameters. Further experiments are under way in this laboratory to enable us to make an accurate comparison between theory and experiment.

ACKNOWLEDGMENTS

We wish to acknowledge many fruitful discussions with J. Hermanson, R. Glosser, J. Kinoshita, and T. J. McMahon.

---

*National Research Council Postdoctoral Research Associate. Present address: Department of Physics, Iowa State University, Ames, Iowa 50010.

[1]E. Burstein, Phys. Rev. 93, 632 (1954).

[2]T. S. Moss, Proc. Phys. Soc. Lond. B 76, 775 (1954).

[3]R. Glosser and B. O. Seraphin, Phys. Rev. 187, 1021 (1969).

[4]D. E. Aspnes and N. Bottka, in *Semiconductors and Semimetals*, edited by R. K. Willardson and A. C. Beer (Academic, New York, 1972), Vol. 9, pp. 468, 472, 484.

[5]This is an arbitrary restriction done for the sake of clarity. The treatment for highly doped p-type materials is analogous.

[6]C. Kittel, in *Quantum Theory of Solids* (Wiley, New York, 1963), p. 186.

[7]R. Glosser, J. E. Fischer, and B. O. Seraphin, Phys. Rev. B 1, 1607 (1970).

[8]J. S. Blakemore, in *Semiconductor Statistics* (Pergamon, New York, 1962), p. 75.

[9]J. M. Ziman, in *Electrons and Phonons, The Theory of Transport Phenomena in Solids* (Clarendon, Oxford, England, 1967), p. 487.

[10]A. S. Grove, B. E. Deal, E. H. Snow, and C. T. Sah, Solid-State Electron. 8, 145 (1964).

[11]D. Pines, in *Elementary Excitations in Solids* (Benjamin, New York, 1964).

[12]D. E. Aspnes and A. Frova, Solid State Commun. 7, 155 (1969).

[13]D. E. Aspnes, J. Opt. Soc. Am. 63, 1380 (1973).

[14]N. Bottka, J. Appl. Phys. 44, 5626 (1973).

[15]E. O. Kane, J. Phys. Chem. Solids 1, 249 (1956).

[16]B. O. Seraphin and H. E. Bennett, in *Semiconductors and Semimetals*, edited by R. K. Willardson and A. C. Beer (Academic, New York, 1967), Vol. 3, pp. 499–543.

[17]R. Y. Hung and E. T. Yon, J. Appl. Phys. 41, 2185 (1970).

[18]C. R. Pidgeon, S. H. Groves, and J. Feinleib, Solid State Commun. 5, 677 (1967).

[19]J. Kinoshita and R. Glosser, Phys. Lett. A 48, 393 (1974).

[20]*American Institute of Physics Handbook*, 3rd ed., edited by D. E. Gray (McGraw-Hill, New York, 1972), p. 6-143.

[21]*American Institute of Physics Handbook*, 3rd ed., edited by D. E. Gray (McGraw-Hill, New York, 1972), p. 6-40.

[22]S. E. Kohn, P. Y. Yu, Y. Petroff, Y. R. Shen, Y. Tsang, and M. L. Cohen, Phys. Rev. B 8, 1477 (1973).

[23]J. N. Zemel, in *Solid State Surface Science*, edited by M. Green (Dekker, New York, 1969), Vol. 1.

[24]C. B. Duke, Phys. Rev. 159, 632 (1967).

[25]G. A. Baraff and J. A. Appelbaum, Phys. Rev. B 5, 475 (1972).

[26]D. C. Tsui, Phys. Rev. B 8, 2657 (1973).

[27]A. Kamgar, P. Kneschaurek, G. Dorda, and J. F. Koch, Phys. Rev. Lett. 32, 1251 (1974).

[28]M. E. Alferieff and C. B. Duke, Phys. Rev. 168, 832 (1968).